

# circCOL12A1 induce epithelial–mesenchymal transition and facilitates oncogenesis in gastric cancer via miR-30b-3p/ZEB1 axis

**Xiaochong Zhang**

Xingtai People's Hospital

**Li Wang**

Xingtai People's Hospital

**Xiaoling Zhao**

Xingtai People's Hospital

**Xiaopeng Tian**

Xingtai People's Hospital

**Qiuxiang Lei**

Xingtai People's Hospital

**Yuandong Li**

Xingtai People's Hospital

**Limin Hui**

Xingtai People's Hospital

**Liangfang Tian**

Xingtai People's Hospital

**Shurui Xie**

Xingtai People's Hospital

**Dengxiang Liu** (✉ [tstcling1@yeah.net](mailto:tstcling1@yeah.net))

Xingtai Institute of Cancer Control, Xingtai People's Hospital

---

## Research Article

**Keywords:** circCOL12A1, miR-30b-3p, gastric cancer, proliferation and migration, epithelial–mesenchymal transition.

**Posted Date:** April 19th, 2022

**DOI:** <https://doi.org/10.21203/rs.3.rs-1560888/v1>

**License:**  This work is licensed under a Creative Commons Attribution 4.0 International License.

[Read Full License](#)

# Abstract

Circular RNAs (circRNAs) play an essential regulatory role in gene expression. Abnormally expressed circRNAs contribute to the occurrence and development of multiple cancers including gastric cancer (GC). However, studies regarding circRNAs in GC remain inadequate. In this study, we used high-throughput screening assays and discovered that circCOL12A1 was significantly increased in GC tissues compared with that in normal gastric tissues. Overexpression of circCOL12A1 enhanced cell proliferation, whereas depletion of circCOL12A1 reduced GC cell migration and epithelial–mesenchymal transition (EMT) by regulating EMT-related gene expression. Mechanistically, circCOL12A1 sponged miR-30b-3p and inhibited miR-30b-3p activity and increased the expression of the EMT-related transcriptional factor, ZEB1. miR-30b-3p expression was lower in GC tissue and correlated with poor survival of GC patients. By contrast, ZEB1 was highly expressed in GC and played a role in promoting GC cell migration and EMT. Furthermore, we confirmed that upregulation of ZEB1 via circCOL12A1-induced inhibition of miR-30b-3p resulted in GC cell proliferation and migration by regulating the EMT process. We demonstrated a pivotal role of circCOL12A1 in regulating proliferation and migration in cancer cells, and the results suggest a therapeutic benefit from targeting the circCOL12A1/miR-30b-3p/ZEB1 pathway in GC.

## 1. Introduction

Gastric cancer (GC) is a common malignant tumor of the upper digestive tract with high a morbidity and mortality rate.[1] Statistics show that the incidence and mortality of GC rank third among malignant tumors for men in developing countries.[2] China has the highest incidence of GC, and new cases and mortality from GC account for approximately half of the worldwide total each year.[3] The onset of GC is relatively insidious, and early symptoms are not always obvious.[4] With the development of modern endoscopy technology, early diagnosis of GC has improved to a certain extent[5]; however, most GCs are still discovered and diagnosed at mid to late stages. At this point, the tumor has migrated, invaded, and metastasized to the surrounding tissues, which affects the overall effectiveness of surgery and post-operative chemotherapy, resulting in a poor prognosis.[6] Tumor cell metastasis is the main cause of cancer-related deaths.[7] Therefore, studying the key genes associated with GC metastasis and exploring the underlying molecular mechanism and its relationship with prognosis and treatment will lead to new strategies to reduce GC mortality.

Circular RNA (circRNA) is a unique type of RNA molecule identified in recent years. Most circRNAs are noncoding RNAs, and a small part can encode small peptide molecules.[8] Studies indicate that circRNAs play an important role in the occurrence and development of tumors.[9] Zhan et al. reported that circAMOTL1L in prostate cancer targets miR-193a-5p to indirectly regulate the expression of PCHAH8, which regulates the epithelial–mesenchymal transition (EMT).[10] CircATP2B1 inhibits the migration and invasion of clear cell renal cell carcinoma (ccRCC) cells, and the estrogen receptor β inhibits the production of circATP2B1, thereby regulating the miR-204-3p/FN1 axis and contributing to the migration of ccRCC cells.[11] Jie et al.[12] found that circMRPS35 inhibits the progression of GC by recruiting KAT7 to control histone modification. Silencing circRACGAP1 sensitizes GC cells to apatinib by targeting miR-

3657 and ATG7 to regulate autophagy.[13] CircLMTK2 acts as a sponge for miR-150-5p and promotes the proliferation and metastasis of GC.[14] Recently, Yuan Dang et al. reported that through a comprehensive analysis of circRNA expression in GC tissue, multiple differentially expressed circRNAs were identified.[15] Although there have been several recent reports of circRNAs in GC, the expression and function of circRNAs in GC remain largely unknown.

The zinc finger E-box binding homeobox 1 (ZEB1, also known as TCF8 and δEF1), which belongs to the family of zinc finger homeodomain transcription factors, is a key transcription factor in the regulation of EMT.[16] The abnormal expression of ZEB1 in many human cancers has been demonstrated, and it is generally believed that it plays a role in promoting cell migration, invasion, and metastasis.[17] In the past few years, *in vitro* and *in vivo* studies have shown that ZEB1 has an unpredictable intrinsic carcinogenic function that affects the occurrence of tumors from an early stage.[18] Studies have found that the expression of ZEB1 is regulated by a variety of signaling pathways and factors including TGF-β, β-catenin, and miRNAs.[19] Xue et al.[19] found that ZEB1, which is upregulated in GC, promotes cell proliferation and migration by regulating Wnt5a and promotes EMT. Murai et al.'s[20] study showed that ZEB1 is positively correlated with the poor prognosis of GC patients; however, the mechanism through which ZEB1 is regulated in GC tissues and its role in tumors remains unclear.

In this study, we confirmed that circCOL12A1 (hsa-circRNA-0077033) was significantly upregulated in GC tissues and cells. Overexpression of circCOL12A1 facilitates the proliferation and migration of GC cells by regulating EMT-related protein levels. Mechanistically, circCOL12A1 binds to and sponges miR-30b-3p in GC cells. This relieves miR-30b-3p repression of the EMT transcriptional factor, ZEB1, thus regulating downstream EMT-related gene expression and attenuating GC progression.

## 2. Methods

*2.1. Clinical samples.* Human primary GC and corresponding normal gastric tissue were collected from the Department of Gastroenterology at the Xingtai People's Hospital. All patients were GC patients from March 2015 to August 2020 and underwent partial gastrectomy. The research protocol was approved by the Ethics Committee of the Xingtai People's Hospital, and written consent was obtained from each patient.

*2.2. Cell lines and transfection.* The normal gastric mucosa epithelial cell line (GES-1) and GC cell lines (AGS, HGC-27, BGC-823, and MGC-803) were purchased from Procell (Wuhan, China). The above-mentioned cells were cultured in RPMI-1640 (Gibco, NY, USA) supplemented with 10% fetal bovine serum (Clark Bio, USA) and 1% penicillin/streptomycin (Gibco, NY, USA). The cells were cultured in a humidified atmosphere of 95% air and 5% CO<sub>2</sub>. Cell transfection was performed as described in the previous [21] by studying using Lipofectamine 2000 (Invitrogen) according to the manufacturer's instructions. The miR-150-5p, miR-205-5p, and miR-30b-3p mimics, mimic-NC, miR-30b-3p inhibitor, inhibitor-NC, si-circCOL12A1, and si-NC were purchased from GenePharma Co., Ltd (Shanghai, China). si-circCOL12A1-F: CAUUUAAAUAUAGCUGUAGTT; si-circCOL12A1-R: CUACAGCUAUUUAAAUGTT; the circCOL12A1

overexpression vector, and luciferase reporter vector were constructed by Biocaring Biotechnology Co., Ltd (Shijiazhuang, China) and confirmed by Sanger sequencing.

**2.3.RNA isolation and qRT-PCR.** The RNAeasy Mini Elute Kit (QIAGEN) was used for total RNA isolation, and the NanoDrop 2000 system was used to measure RNA concentration and quality. Complementary DNA was synthesized using the M-MLV First Strand Kit (Life Technologies) with random hexamer primers and diluted cDNA 5- to 10-fold according to the concentration. MicroRNA reverse transcription was conducted using the miScriptIIRT kit (QIAGEN GmbH, D-40724 Hilden, GERMANY) following the manufacturer's protocol. Platinum SYBR Green qPCR Super Mix UDG kit (Invitrogen) was used for quantitative real-time PCR (qRT-PCR) analysis along with the ABI 7500 FAST System (Life Technologies). GAPDH was used as an internal reference gene for standardization. The  $2^{-\Delta\Delta Ct}$  formula was used to calculate relative gene expression as described previously [21]. The primers used were as follows:  
COL12A1-F: CAAGCTCATTGTAGTCGACATCAGCC; COL12A1-R: GTCTTGACTTGGGAGAGCGGC;  
circCOL12A1-F: CCTGTAGGAGGTGGCTGC; circCOL12A1-R: GGTCTTCCCCAGCTACTCAGC; miR-29a-5p:  
GCGACTGATTCTTTGGTGTTC; miR-30b-3p: GGCCCTGGGAGGTGGATGTTAC; miR-133a-3p:  
TTTGGTCCCCTCAACCAGC; miR-193b-3p: AACTGGCCCTCAAAGTCCCG; miR-200c-3p:  
TAATACTGCCGGGTAATGATG; miR-338-3p: CCAGCATCAGTGATTTGTTG; miR-432-3p:  
CTGGATGGCTCCTCCATGTC; miR-605-3p: GGCAGAAAGGCACATGAGATTAG; miR-579-3p:  
GGCTTCATTGGTATAAACCGCG; miR-877-5p: GTAGAGGAGATGGCGCAGG; miR-1178-5p:  
GGCAGGGTCAGCTGAGCATG.

### *Microarray*

Microarray was used to detect the circRNAs expression as previously described[22]. Total RNAs from five GC tissues and corresponding normal gastric tissues were extracted and digested with RNase R (Epicentre, Inc., Madison, WI, USA) to remove linear RNAs and thus enrich circRNAs. The enriched circRNAs were amplified and transcribed into fluorescent cRNA using a random priming method (Arraystar Super RNA Labeling Kit; Arraystar). The labeled cRNAs were purified using an RNeasy Mini Kit (Qiagen, Venlo, Netherlands). The concentration and specific activity of the labeled cRNAs (pmol Cy3/ $\mu$ g cRNA) were measured using a NanoDrop ND-1000 (Thermo Scientific, Waltham, MA, USA). One microgram of each labeled cRNA was fragmented by adding 5  $\mu$ l of 10 $\times$  Blocking Agent and 1  $\mu$ l of 25 $\times$  Fragmentation Buffer; after heating the mixture at 60°C for 30 min, 25  $\mu$ l of 2 $\times$  Hybridization Buffer was added to dilute the labeled cRNA. Next, 50  $\mu$ l of hybridization solution was dispensed into the gasket slide and assembled to the circRNA expression microarray slide. The slides were incubated for 17 h at 65°C in an Agilent hybridization oven (Agilent Technologies, Santa Clara, CA, USA). The hybridized arrays were washed, fixed, and scanned using the Agilent Scanner G2505C. Agilent Feature Extraction software (version 11.0.1.1) was used to analyze the acquired array images. Quantile normalization and subsequent data processing were performed using the GeneSpring GX v11.5.1 software package (Agilent Technologies).

**2.4. Western blot analysis.** Western blot analysis of cells and tissues was conducted as previously described[22, 23]. RIPA lysis buffer was used to extract proteins from cultured cells and frozen tissues. A modified Bradford method was used for protein quantitation, and an equal amount of protein was loaded onto the gel. Proteins were separated by SDS-PAGE and electrotransferred to polyvinylidene fluoride membranes (Millipore). The membranes were blocked with 5% milk for 2 h and incubated with primary antibody overnight at 4°C. The following antibodies were used: ZEB1 (1:1000, ab245283), E-cadherin (1:1000, 20874-1-AP), vimentin (Vim; 1:1000, 10366-1-AP), CDK6 (1:1000, 14052-1-AP), MMP2 (1:1000, 10373-2-AP), and β-actin (1:1000, sc-47778). The HRP-labeled secondary antibody (1:10000, Rockland) was incubated with the membranes for 1 h at room temperature. Immobilon™ Western chemiluminescence HRP substrate (Millipore) was used to develop the membrane and detected by ECL (enhanced chemiluminescence) Fuazon Fx (Vilber Lourmat). FusionCapt Advance Fx5 software (Vilber Lourmat) was used to capture and process the images. All experiments were repeated three times.

**2.5. Target prediction.** To identify potential miRNAs of circCOL12A1 as methods of Z. Yang et al. 2021[21], we used the miRanda ([www.microrna.org](http://www.microrna.org)), RNAhybrid (<http://bibiserv.techfak.uni-bielefeld.de/rnahybrid/submission.html>), and RNA22 (<https://cm.jefferson.edu/rna22/Interactive/>). For predicting the target gene of miRNA, we used Targetscan (<http://www.targetscan.org>).

**2.6. Luciferase assay.** For the luciferase assay we followed the methods of Z. Yang et al. 2021 [21]. The HGC-27 cells were seeded into a 12-well plate. For the circCOL12A1-miRNA luciferase assay, HGC-27 cells were co-transfected with miRNA mimics or NC mimics and the circCOL12A1-luciferase reporter gene or empty vector. For the miR-30b-3p-ZEB1 luciferase assay, HGC-27 cells were transfected with the miRNA-194-3p mimic or NC mimic and ZEB1-3'UTR luciferase reporter (wt or mut). A dual Glo luciferase assay system (Promega, Madison, WI) (LB955, Berthold Technologies) with flash and luminescence was used to measure luciferase activity.

**2.7. Oligo pull-down.** HGC-27 cells were incubated with a biotin (bio)-labeled oligonucleotide probe for circCOL12A1 (Bio-5'-CTCTCACTGAAACAGAAATGTTCCGAATAAC, GenePharma Co., Shanghai) at 37°C for 4 h. M-280 Streptavidin Dynabeads (Life Technologies) were added per 100 pmol of biotin-DNA oligonucleotide, and the mixture was rotated at 37°C for 30 min. The magnetic beads were captured using a magnet (Life Technologies) and washed five times. Each experiment was repeated three times as previous description [21].

**2.8. Transwell assay.** The transwell assay was performed as previous description[21]. A Transwell chamber with an 8 μm pore size (Costar, Massachusetts) was used to detect the migration ability of HGC-27 cells. In short,  $3 \times 10^4$  cells/well of HGC-27 cells was seeded into the upper compartment with a serum-free medium. Medium containing 10% FBS was added to the lower compartment. After culturing at 37°C and 5% CO<sub>2</sub> for 24 h, the cells were treated as indicated. The cells with a higher migration ability on the upper side of the chamber migrated to the lower chamber. The number of migrating cells was counted in three randomly selected areas by microscopy.

**2.9. MTT assay.** Cell viability was measured using an MTT [3-(4,5-dimethylthiazol-2-yl)-2,5-diphenyltetrazolium bromide] assay. Briefly, HGC-27 and AGS cells were seeded into 96-well plates. Cells were transfected with the indicated vector for 24 h; a 20 µL MTT reagent (5 mg/mL; Sigma-Aldrich) was added to each well and incubated for 3 to 4 h. A microplate reader (Thermo Fisher, USA) was used to measure the absorbance.

**2.10. Colony formation assay.** For the colony formation assay we followed the methods of Z. Yang et al. 2021[21], 100 cultured cells/well were seeded into six-well plates, cultured for 1 week, and were then fixed in glacial acetic acid/methanol solution. Then, 0.5% crystal violet was used to stain the colonies. Colony numbers were counted under a microscope.

**2.11. ChIP assay.** The chromatin immunoprecipitation (ChIP) assay was conducted as previously described [24]. Briefly, Caki-1 cells were treated with formaldehyde. The cross-linked chromatin was prepared and sonicated to an average size of 400–600 bp. The samples were diluted 10-fold and then precleared with protein A-agarose/salmon sperm DNA for 30 min at 4°C. The DNA fragments were immunoprecipitated overnight at 4°C with anti-MAZ or anti-IgG antibodies. After reversing the crosslinks, MAZ occupancy on the MAP2K2 promoter was examined. The results were determined via qRT-PCR. The ChIP primer sequences were as follows: MAP2K2-prom-F1: GTGGTAAGGCAAGCGAGGGCG; MAP2K2-prom-R1: AGGGGAGGGCGGCCACAAG; MAP2K2-prom-F2: GGTTCTCTCAGCCCCAGCCTG; MAP2K2-prom-R2: GGCGCCCTCGCTTGCCTTAC; MAP2K2-prom-F3: CCATCCTGGCTAACACGGTG; and MAP2K2-prom-R3: GGAGTGCAGTGGTGCATCTC.

**2.12. Statistical analysis.** Data were presented as the mean ± SEM. A Student's *t* test was used to analyze differences between the two groups. Spearman's correlation analysis was used to determine correlation coefficients. P < 0.05 was considered statistically significant. GraphPad Prism 7.0 software was used for the analyses (GraphPad Software).

### 3. Results

**3.1. CircCOL12A1 is a stable highly expressed circRNA in GC tissues.** To explore the molecular mechanisms underlying circRNA role in GC, we first used circular RNA microarrays to obtain circRNA profiles in GC tissues. Five pairs of samples were taken from the two different areas. After scanning and normalization, 1238 circRNAs were found to be differentially expressed between GC tissues and normal gastric tissues (> 2.0 fold change in expression level; P < 0.05). Among them, 1073 circRNAs were upregulated and 874 were downregulated in GC tissues (Supplementary Table 1). As shown in Fig. 1A, unsupervised hierarchical clustering analysis of circRNA profiling was able to clearly differentiate the GC tissues from the normal tissues. To further confirm the microarray data, Ten differentially expressed circRNAs were selected to verify their expressions in GC and normal tissues by using qRT-PC. Then, we used a divergent primers to amplify circCOL12A1 (hsa-circRNA-0077033) formed by head-to-tail splicing and confirmed the presence of this circRNAs, which was high expression in GC tissues (Fig. 1C). In order to confirm whether the circCOL12A1 was upregulated commonly in GC tissues, a large number of clinical

samples were used to verify the expression of circCOL12A1 in GC tissues ( $n = 52$ ) and corresponding normal tissues ( $n = 52$ ). The result indicated that the level of circCOL12A1 was significantly increased in GC tissues compared with that in normal gastric tissues (Fig. 1D). Furthermore, fluorescence *in situ* hybridization revealed that circCOL12A1 was upregulated in GC tissues and was predominately localized in the cytoplasm (Fig. 1E and F). Besides, we determined that the circCOL12A1 was resistant to RNase R treatment in HGC-27 cells, whereas the host gene COL12A1 mRNA was sensitive (Fig. 1G). A correlation analysis revealed that the circCOL12A1 level was significantly associated with tumor size and node invasion number, but not with other clinicopathologic factors including age, sex, and T stage (Table 1). These findings indicate that circCOL12A1 is overexpressed in GC, and the upregulation of circCOL12A1 may be correlated with GC development.

Table 1  
Clinicopathological Characteristics

Characteristics	Number of patients (%)	circCOL12A1 expression		
		Low (%)	High (%)	Pvalue
		26	26	
<b>Age</b>				
≤ 50 years	25	13 (52.00)	12 (48.00)	0.781
> 50 years	27	13 (48.15)	14 (51.85)	
<b>Gender</b>				
Male	37	19 (51.35)	18 (48.65)	0.760
Female	15	7(46.67)	8 (53.33)	
<b>Tumor size</b>				
≤ 4 cm	20	14 (70.00)	6(30.00)	0.023
> 4cm	32	12 (37.50)	20 (62.50)	
<b>T stage</b>				
T <sub>3</sub> or lower	7	4 (57.14)	3 (42.86)	0.670
T <sub>4a</sub>	35	16 (45.71)	19 (54.29)	
T <sub>4b</sub>	10	6 (60.00)	4 (40.00)	
<b>Nods invasion</b>				
Less than 16	33	20(60.61)	13 (39.39)	0.044
16 or more	19	6 (31.58)	13 (68.42)	
<b>Lauren's</b>				
<b>Classification</b>				
Intestinal and mixed	25	12 (48.00)	13(52.00)	0.781
Diffuse	27	14 (51.85)	13(48.15)	

3.2. *CircCOL12A1 facilitates the proliferation and migration of GC cells in vitro.* To investigate the function of circCOL12A1 in GC, we first compared circCOL12A1 expression between a normal human gastric epithelial cell line (GES-1) and four GC cell lines (AGS, HGC-27, BGC-823, and MGC-803). The results showed that HGC-27 cells exhibited higher circCOL12A1 expression levels, whereas AGS cells had

relative lower levels (Fig. 2A). In subsequent experiments, we chose HGC-27 cells for circCOL12A1 knockdown and AGS cells for circCOL12A1 overexpression. Next, qRT-PCR was used to confirm knockdown efficiency by using si-RNA in HGC-27 cell lines (Fig. 2B). Additionally, AGS cells were transfected with a circCOL12A1 overexpression plasmid, indicating that circCOL12A1 may be upregulated in AGS cells (Fig. 2C). We then determined cell viability using an MTT assay. The results showed that circCOL12A1 knockdown resulted in the inhibition of HGC-27 cell growth, whereas overexpression of circCOL12A1 promoted cell proliferation in AGS cells (Fig. 2D and E). Subsequently, transwell assays were conducted to detect the effect of circCOL12A1 on GC cell migration. As shown in Fig. 2F to 2I, depletion of circCOL12A1 suppressed the migration ability of HGC-27 cells compared with the negative control, whereas overexpression of circCOL12A1 significantly increased the migratory ability of AGS cells. These findings suggest that circCOL12A1 contributes to GC cell proliferation and migration.

**3.3. circCOL12A1 promotes EMT by regulating EMT-related genes.** Because EMT is a critical process in cell proliferation and migration[25, 26], we explored the relationship between circCOL12A1 and EMT. We then measured the expression of the EMT-related genes, E-cadherin, Vim, and migration-related protein matrix metallopeptidase 2 (MMP2). The results indicated that the depletion of circCOL12A1 in HGC-27 cells significantly increased the expression of E-cadherin and reduced the expression of MMP2 and Vim (Fig. 3A and B). By contrast, overexpression of circCOL12A1 in AGS cells markedly reduced E-cadherin expression but increased MMP2 and Vim protein levels (Fig. 3C and D). Similarly, immunofluorescence staining verified that knockdown of circCOL12A1 in HGC-27 cells significantly increased the expression of E-cadherin and reduced the expression of Vim (Fig. 3E). Conversely, overexpression of circCOL12A1 decreased the expression of E-cadherin in the cell membrane and increased the level of Vim (Fig. 3F). Together, these findings suggest that circCOL12A1 promotes the EMT phenotype in GC cells by regulating the expression of MMP2, E-Cadherin, and Vim.

**3.4. CircCOL12A1 serves as a miRNA sponge for miR-30b-3p in GC cells.** Because studies have shown that circRNAs function as miRNAs sponges, we sought to identify the corresponding miRNAs of circCOL12A1. Using prediction programs, miRanda, RNA22, and RNAhybrid, we found seven putative miRNAs that bind to circCOL12A1 (Fig. 4a). To examine the interaction of miRNAs and circCOL12A1, we used a biotin-labeled circCOL12A1 probe to perform a pull-down assay and used qRT-PCR to measure the pull-down efficiency. As shown in Fig. 4B, the pull-down efficiency of circCOL12A1 was significantly higher in circCOL12A1-overexpressing cells. The candidate miRNAs were measured via qRT-PCR in the precipitates that were pulled down with a circCOL12A1 biotin-labeled probe. The results showed enrichment of miR-150-5p, miR-30b-3p, and miR-181-5p in the precipitates (Fig. 4C). Furthermore, full-length circCOL12A1 was sub-cloned into a psiCHECK-2 luciferase vector, and the reporter construct was co-transfected with miRNA mimics into HGC-27 cells. The results showed that miR-30b-3p significantly reduced luciferase activity by 45%, but miR-150-5p and miR-181-5p had no effect, which suggests that miR-194-5p was specifically bound to circCOL12A1 (Fig. 4D). Another study reported that the expression of miR-30b-3p is downregulated in cancer tissues[27] and a qRT-PCR analysis revealed that miR-30b-3p levels were lower in GC tissues than in normal gastric tissues (Fig. 4E). A correlation analysis revealed a negative correlation between miR-30b-3p and circCOL12A1 expression levels in GC tissues (Fig. 4F).

Additionally, the TCGA database also confirmed that lower miR-194-5p levels in GC patients were associated with poor overall survival (Fig. 4G). These results suggest that circCOL12A1 binds to miR-30b-3p in GC cells.

**3.5. miR-30b-3p inhibits GC cell EMT by targeting the ZEB1 gene 3'UTR.** Previous studies have shown that miR-30b-3p is involved in cell proliferation and migration[28, 29]; therefore, we determined whether miR-30b-3p plays a role in GC cell EMT. First, HGC-27 cells were transfected with a miR-30b-3p inhibitor or mimic, and EMT-related marker genes were examined via western blot analysis. The results showed that the miR-30b-3p inhibitor promoted ZEB1 and Vim protein expression and suppressed E-cadherin protein levels, whereas miR-30b-3p mimic yielded the opposite result (Fig. 5A and B). A computer-based sequence analysis showed that there is a putative miR-30b-3p binding site in ZEB1 3'UTR (Fig. 5C). Subsequently, a luciferase analysis revealed that miR-30b-3p mimics reduced wild-type 3'UTR luciferase activity but did not affect the luciferase activity of the mutant 3'UTR (Fig. 5D). To determine whether miR-30b-3p affects ZEB1 expression, we performed a qRT-PCR assay. As shown in Fig. 5E, overexpression of miR-30b-3p downregulated ZEB1, whereas knockdown by miR-30b-3p upregulated ZEB1 mRNA in HGC-27 cells. Furthermore, the qRT-PCR analysis indicated that the ZEB1 mRNA level was higher in GC tissues than in normal gastric tissues (Fig. 5F). The upregulated-ZEB1 exhibited a negative correlation with miR-30b-3p in GC tissues (Fig. 5G). Additionally, the TCGA database also confirmed that high levels of ZEB1 in patients with GC were associated with poor overall survival (Fig. 5H). Together, these findings indicate that miR-30b-3p directly inhibits ZEB1 expression and regulates GC cell EMT in GC cells.

**3.6. The circCOL12A1/miR-30b-3p/ZEB1 axis regulates GC cell proliferation and migration.** To identify a role for circCOL12A1/miR-30b-3p/ZEB1 in GC cell proliferation and migration, we conducted rescue experiments. First, AGS cells were transfected with the overexpressing circCOL12A1 vector and miR-30b-3p mimic or co-transfected with both together. Western blot analysis was used to detect EMT and proliferation-related protein expression. The results showed that circCOL12A1 increased Vim, ZEB1, and CDK6 protein levels and suppressed E-cadherin protein expression. However, the effect of circCOL12A1 on the expression of these proteins was partly reversed by miR-30b-3p mimic and circCOL12A1 co-transfected AGS cells (Fig. 6A and B). Additionally, a cell viability assay showed that overexpression of circCOL12A1 in AGS cells markedly elevated cell growth compared with the empty vector control and reversed the inhibitory effects of miR-30b-3p overexpression on cell proliferation (Fig. 6C). Similarly, overexpression of ZEB1 enhanced AGS cell proliferation, whereas circCOL12A1 knockdown reversed the effects of ZEB1 on proliferation (Fig. 6D). Furthermore, overexpression of circCOL12A1 significantly promoted cell migration compared with the empty vector and reversed the inhibitory effect of miR-30b-3p overexpression on cell migration (Fig. 6E and F). Together, these findings confirm that circCOL12A1/miR-30b-3p/ZEB1 axis regulates GC cell proliferation and migration.

## 4. Discussion

In the present study, we investigated the biological role of the circCOL12A1/miR-30b-3p/ZEB1 axis in modulating GC oncogenesis. First, the high-throughput circRNA chip revealed that circCOL12A1 expression was significantly increased in GC tissues from clinical samples, and higher levels of circCOL12A1 in patients were associated with tumor size and node invasion number. Second, circCOL12A1 appeared to function as an oncogene as it promoted GC proliferation and migration *in vitro*. Third, circCOL12A1 positively regulated ZEB1 expression in GC cells. Mechanistically, circCOL12A1 induces the EMT transcription factor, ZEB1, expression by sponging miR-30b-3p, which directly targets the ZEB1 gene 3'UTR. Our findings indicate that the circCOL12A1/miR-30b-3p/ZEB1 pathway plays a role in the proliferation and migration in GC.

EMT is one of the preconditions for tumor cell migration and invasion. EMT refers to the loss of the ability of epithelial cells to adhere to adjacent cells and the extracellular matrix which enhances migration, invasion, and metastasis of mesenchymal cells.[30, 31] The EMT process is regulated by complex factors including cytokines, growth factors, signal pathways, transcription factors, and the tumor microenvironment.[32] For example, the EMT-related transcription factors Snail1, Snail2, ZEB1/ZEB2, TCF3, and Kruppel-like factor 8 (KLF8) can bind to the promoter of the epithelial marker, E-cadherin, to inhibit its transcription. The transcription factors, Twist, Goosecoid, TCF4, homeobox Protein SIX1, and forkhead protein C2 (FOXC2), indirectly inhibit E-cadherin expression.[33, 34] In addition to E-cadherin, these transcription factors also inhibit the transcription of other connexins including tight junction proteins and desmosomal proteins. EMT is also involved in multiple signaling pathways (TGF- $\beta$ , FGF, PDGF, EGF, HGF, IGF, ER $\alpha$ , Wnt / $\beta$ -catenin, and Notch) and during hypoxic conditions.[35–37] These signal transduction pathways ultimately activate the transcription of EMT-related transcription factors. Additionally, noncoding RNA also plays an important regulatory role in the EMT process. The miR-200 family, miR-101, and miR-506, controls EMT by regulating the expression of EMT-related transcription factors or EMT-related genes.[35] MiR-27b and miR-34a were shown to inhibit EMT by targeting ZEB1, thereby enhancing the sensitivity of PCa cells to docetaxel.[38] The silencing of miR-193a-5p increased the chemo-sensitivity of PCa cells to docetaxel.[39] Yang et al. found that the expression of circAMOTL1L is downregulated in human PCa. The downregulation of circAMOTL1L resulted in a decrease in the expression of the E-cadherin and an upregulation in the expression of the mesenchymal marker molecule, Vim, to promote the migration and invasion of EMT and PCa cells.[22] In the present study, we found that upregulation of circCOL12A1 promotes the proliferation and migration of GC cells by regulating EMT-related protein levels. Overexpression of circCOL12A1 dramatically reduced E-cadherin but increased MMP2 and Vim protein levels. CircCOL12A1 binds to and sponges miR-30b-3p in GC cells. This relieves miR-30b-3p repression of the EMT transcriptional factor, ZEB1, which is a key EMT-related transcription factor.

Because of the rapid development of high-throughput sequencing technology and bioinformatics, researchers have identified a large number of circRNAs in mammalian cells.[40] Most studies have focused on circRNA as a regulator of parental gene transcription, alternative splicing, and sponging miRNA[41] Additionally, circRNAs interact with proteins to regulate expression and activity.[42] Most of these circRNAs are noncoding RNAs; however, several have been shown to encode functional proteins.

[43] Studies have found that the abnormal expression of circRNAs occurs in a variety of human diseases including GC.[40] Moreover, some circRNAs with biological functions are continuously being reported, including those involved in cell proliferation, apoptosis, migration, and invasion.[40] CircNRIP1 acts as a microRNA-149-5p sponge and promotes GC progression through the AKT1/mTOR pathway.[44] Upregulation of circRNA\_100876 promotes the growth, migration, and invasion of GC cells through miR-665/YAP1 signaling.[45] CircRNA\_0023642 facilitates the migration and invasion of GC cells by regulating EMT.[46] The present study analyzed the expression profiles of circRNAs in multiple GC tissues and discovered that hsa\_circ\_0006401, hsa\_circ\_0077033, hsa\_circ\_0044518, hsa\_circ\_0044516, hsa\_circ\_0081090, hsa\_circ\_0058132, and many other circRNAs are abnormally expressed in GC tissues. After verification using clinical samples, hsa\_circ\_0006401 (circCOL12A1) was found to be upregulated in GC tissues and cells. We further found that upregulated circCOL12A1 significantly increases the proliferation and migration of GC cells and enhances the progression of GC by regulating the expression of ZEB1 and EMT. In summary, our findings reveal that the circCOL12A1/miR-30b-3p/ZEB1 axis plays an important role in GC cell migration and EMT, correlates with GC progression, and provides a new potential therapeutic target for GC.

## Declarations

### Ethics Approval and Consent to Participate

The study was approved by the Ethics Committee of the Xingtai People's Hospital and written consent was obtained from each patient.

### Consent for Publication

Not applicable

### Funding

This study was partially supported by The Key Research and Development Project of Hebei Province (No. 182777122D).

### Availability of Data and Materials

The data that support the findings of this study are available from the corresponding author upon reasonable request.

### Author Contributions

Study conception and design: Xiaochong Zhang and Li Wang. Acquisition of data: Xiaochong Zhang, Li Wang, Xiaoling Zhao, Xiaopeng Tian, and Qiuxiang Lei. Analysis and interpretation of data: Xiaochong Zhang, Dengxiang Liu. Drafting of the manuscript: Xiaochong Zhang, and Li Wang, Final approval of the submitted manuscript: all authors.

Not applicable.

### Conflict of Interest Statement

All authors declare no conflict of interest.

## References

1. Smyth EC, Nilsson M, Grabsch HI, van Grieken NC, Lordick F: **Gastric cancer**. Lancet 2020, **396**(10251):635–648.
2. Goncalves WGE, Dos Santos MHP, Lobato FMF, Ribeiro-Dos-Santos A, de Araujo GS: **Deep learning in gastric tissue diseases: a systematic review**. BMJ Open Gastroenterol 2020, **7**(1):e000371.
3. Li Y, Sui X, Su Z, Yu C, Shi X, Johnson NL, Chu F, Li Y, Li K, Ding X: **Meta-Analysis of Paclitaxel-Based Chemotherapy Combined With Traditional Chinese Medicines for Gastric Cancer Treatment**. Front Pharmacol 2020, **11**:132.
4. Ang TL, Fock KM: **Clinical epidemiology of gastric cancer**. Singapore medical journal 2014, **55**(12):621–628.
5. Johnston FM, Beckman M: **Updates on Management of Gastric Cancer**. Current oncology reports 2019, **21**(8):67.
6. D'Ugo D, Agnes A, Grieco M, Biondi A, Persiani R: **Global updates in the treatment of gastric cancer: a systematic review. Part 2: perioperative management, multimodal therapies, new technologies, standardization of the surgical treatment and educational aspects**. Updates Surg 2020.
7. Astudillo P: **Wnt5a Signaling in Gastric Cancer**. Front Cell Dev Biol 2020, **8**:110.
8. Huang A, Zheng H, Wu Z, Chen M, Huang Y: **Circular RNA-protein interactions: functions, mechanisms, and identification**. Theranostics 2020, **10**(8):3503–3517.
9. Chen B, Huang S: **Circular RNA: An emerging non-coding RNA as a regulator and biomarker in cancer**. Cancer Lett 2018, **418**:41–50.
10. Yang Z, Qu CB, Zhang Y, Zhang WF, Wang DD, Gao CC, Ma L, Chen JS, Liu KL, Zheng B *et al*: **Dysregulation of p53-RBM25-mediated circAMOTL1L biogenesis contributes to prostate cancer progression through the circAMOTL1L-miR-193a-5p-Pcdha pathway**. Oncogene 2018.
11. Han Z, Zhang Y, Sun Y, Chen J, Chang C, Wang X, Yeh S: **ERbeta-mediated alteration of circATP2B1 and miR-204-3p signaling promotes invasion of clear cell renal cell carcinoma**. Cancer Res 2018.
12. Jie M, Wu Y, Gao M, Li X, Liu C, Ouyang Q, Tang Q, Shan C, Lv Y, Zhang K *et al*: **CircMRPS35 suppresses gastric cancer progression via recruiting KAT7 to govern histone modification**. Mol Cancer 2020, **19**(1):56.
13. Ma L, Wang Z, Xie M, Quan Y, Zhu W, Yang F, Zhao C, Fan Y, Fang N, Jiang H *et al*: **Silencing of circRACGAP1 sensitizes gastric cancer cells to apatinib via modulating autophagy by targeting miR-3657 and ATG7**. Cell Death Dis 2020, **11**(3):169.

14. Mautz WJ, Kleinman MT, Phalen RF, Crocker TT: **Effects of exercise exposure on toxic interactions between inhaled oxidant and aldehyde air pollutants.** J Toxicol Environ Health 1988, **25**(2):165–177.
15. Dang Y, Ouyang X, Zhang F, Wang K, Lin Y, Sun B, Wang Y, Wang L, Huang Q: **Circular RNAs expression profiles in human gastric cancer.** Sci Rep 2017, **7**(1):9060.
16. Wu HT, Zhong HT, Li GW, Shen JX, Ye QQ, Zhang ML, Liu J: **Oncogenic functions of the EMT-related transcription factor ZEB1 in breast cancer.** Journal of translational medicine 2020, **18**(1):51.
17. Lindner P, Paul S, Eckstein M, Hampel C, Muenzner JK, Erlenbach-Wuensch K, Ahmed HP, Mahadevan V, Brabertz T, Hartmann A *et al*: **EMT transcription factor ZEB1 alters the epigenetic landscape of colorectal cancer cells.** Cell Death Dis 2020, **11**(2):147.
18. Krebs AM, Mitschke J, Lasierra Losada M, Schmalhofer O, Boerries M, Busch H, Boettcher M, Mougiakakos D, Reichardt W, Bronsert P *et al*: **The EMT-activator Zeb1 is a key factor for cell plasticity and promotes metastasis in pancreatic cancer.** Nature cell biology 2017, **19**(5):518–529.
19. Caramel J, Ligier M, Puisieux A: **Pleiotropic Roles for ZEB1 in Cancer.** Cancer research 2018, **78**(1):30–35.
20. Murai T, Yamada S, Fuchs BC, Fujii T, Nakayama G, Sugimoto H, Koike M, Fujiwara M, Tanabe KK, Kodera Y: **Epithelial-to-mesenchymal transition predicts prognosis in clinical gastric cancer.** Journal of surgical oncology 2014, **109**(7):684–689.
21. Ren LX, Qi JC, Zhao AN, Shi B, Zhang H, Wang DD, Yang Z: **Myc-associated zinc-finger protein promotes clear cell renal cell carcinoma progression through transcriptional activation of the MAP2K2-dependent ERK pathway.** Cancer cell international 2021, **21**(1):323.
22. Yang Z, Qu CB, Zhang Y, Zhang WF, Wang DD, Gao CC, Ma L, Chen JS, Liu KL, Zheng B *et al*: **Dysregulation of p53-RBM25-mediated circAMOTL1L biogenesis contributes to prostate cancer progression through the circAMOTL1L-miR-193a-5p-Pcdha pathway.** Oncogene 2019, **38**(14):2516–2532.
23. Qi JC, Yang Z, Lin T, Ma L, Wang YX, Zhang Y, Gao CC, Liu KL, Li W, Zhao AN *et al*: **CDK13 upregulation-induced formation of the positive feedback loop among circCDK13, miR-212-5p/miR-449a and E2F5 contributes to prostate carcinogenesis.** Journal of experimental & clinical cancer research: CR 2021, **40**(1):2.
24. Zhang YP, Liu KL, Wang YX, Yang Z, Han ZW, Lu BS, Qi JC, Yin YW, Teng ZH, Chang XL *et al*: **Down-regulated RBM5 inhibits bladder cancer cell apoptosis by initiating an miR-432-5p/beta-catenin feedback loop.** FASEB J 2019, **33**(10):10973–10985.
25. Qin A, Wu J, Zhai M, Lu Y, Huang B, Lu X, Jiang X, Qiao Z: **Axin1 inhibits proliferation, invasion, migration and EMT of hepatocellular carcinoma by targeting miR-650.** American journal of translational research 2020, **12**(3):1114–1122.
26. Lu J, Li D, Zeng Y, Wang H, Feng W, Qi S, Yu L: **IDH1 mutation promotes proliferation and migration of glioma cells via EMT induction.** Journal of BUON: official journal of the Balkan Union of Oncology 2019, **24**(6):2458–2464.

27. Yi L, Ouyang L, Wang S, Li SS, Yang XM: **Long noncoding RNA PTPRG-AS1 acts as a microRNA-194-3p sponge to regulate radiosensitivity and metastasis of nasopharyngeal carcinoma cells via PRC1.** Journal of cellular physiology 2019, **234**(10):19088–19102.
28. Abuduaini R, Miao X, Xu J, Che L, Zhou W, Guo Z, Sun J: **MicroRNA-194-3p inhibits the metastatic biological behaviors of spinal osteosarcoma cells by the repression of matrix metallopeptidase 9.** Int J Clin Exp Pathol 2018, **11**(11):5257–5264.
29. Tian Z, Wang R, Zhang X, Deng B, Mi C, Liang T, Ling Y, Li H, Zhang H: **Benzo[a]Pyrene-7, 8-Diol-9, 10-Epoxide Suppresses the Migration and Invasion of Human Extravillous Trophoblast Swan 71 Cells Due to the Inhibited Filopodia Formation and Down-Regulated PI3K/AKT/CDC42/PAK1 Pathway Mediated by the Increased miR-30b-3p.** Toxicological sciences: an official journal of the Society of Toxicology 2018, **166**(1):25–38.
30. Lee HM, Hwang KA, Choi KC: **Diverse pathways of epithelial mesenchymal transition related with cancer progression and metastasis and potential effects of endocrine disrupting chemicals on epithelial mesenchymal transition process.** Molecular and cellular endocrinology 2017, **457**:103–113.
31. Odero-Marah VA, Wang R, Chu G, Zayzafoon M, Xu J, Shi C, Marshall FF, Zhau HE, Chung LW: **Receptor activator of NF-kappaB Ligand (RANKL) expression is associated with epithelial to mesenchymal transition in human prostate cancer cells.** Cell Res 2008, **18**(8):858–870.
32. Castellanos JA, Merchant NB, Nagathihalli NS: **Emerging targets in pancreatic cancer: epithelial-mesenchymal transition and cancer stem cells.** OncoTargets and therapy 2013, **6**:1261–1267.
33. Yang J, Weinberg RA: **Epithelial-mesenchymal transition: at the crossroads of development and tumor metastasis.** Developmental cell 2008, **14**(6):818–829.
34. Peinado H, Olmeda D, Cano A: **Snail, Zeb and bHLH factors in tumour progression: an alliance against the epithelial phenotype?** Nature reviews Cancer 2007, **7**(6):415–428.
35. Guo F, Parker Kerrigan BC, Yang D, Hu L, Shmulevich I, Sood AK, Xue F, Zhang W: **Post-transcriptional regulatory network of epithelial-to-mesenchymal and mesenchymal-to-epithelial transitions.** Journal of hematology & oncology 2014, **7**:19.
36. Zhang L, Huang G, Li X, Zhang Y, Jiang Y, Shen J, Liu J, Wang Q, Zhu J, Feng X *et al*: **Hypoxia induces epithelial-mesenchymal transition via activation of SNAI1 by hypoxia-inducible factor – 1alpha in hepatocellular carcinoma.** BMC cancer 2013, **13**:108.
37. Kalluri R, Weinberg RA: **The basics of epithelial-mesenchymal transition.** The Journal of clinical investigation 2009, **119**(6):1420–1428.
38. Zhang G, Tian X, Li Y, Wang Z, Li X, Zhu C: **miR-27b and miR-34a enhance docetaxel sensitivity of prostate cancer cells through inhibiting epithelial-to-mesenchymal transition by targeting ZEB1.** Biomedicine & pharmacotherapy = Biomedecine & pharmacotherapie 2018, **97**:736–744.
39. Yang Z, Chen JS, Wen JK, Gao HT, Zheng B, Qu CB, Liu KL, Zhang ML, Gu JF, Li JD *et al*: **Silencing of miR-193a-5p increases the chemosensitivity of prostate cancer cells to docetaxel.** Journal of experimental & clinical cancer research: CR 2017, **36**(1):178.

40. Li R, Jiang J, Shi H, Qian H, Zhang X, Xu W: **CircRNA: a rising star in gastric cancer.** Cellular and molecular life sciences: CMLS 2020, **77**(9):1661–1680.
41. Salzman J: **Circular RNA Expression: Its Potential Regulation and Function.** Trends in genetics: TIG 2016, **32**(5):309–316.
42. Du WW, Zhang C, Yang W, Yong T, Awan FM, Yang BB: **Identifying and Characterizing circRNA-Protein Interaction.** Theranostics 2017, **7**(17):4183–4191.
43. Wu P, Mo Y, Peng M, Tang T, Zhong Y, Deng X, Xiong F, Guo C, Wu X, Li Y *et al*: **Emerging role of tumor-related functional peptides encoded by lncRNA and circRNA.** Mol Cancer 2020, **19**(1):22.
44. Zhang X, Wang S, Wang H, Cao J, Huang X, Chen Z, Xu P, Sun G, Xu J, Lv J *et al*: **Circular RNA circNRIP1 acts as a microRNA-149-5p sponge to promote gastric cancer progression via the AKT1/mTOR pathway.** Mol Cancer 2019, **18**(1):20.
45. Lin X, Huang C, Chen Z, Wang H, Zeng Y: **CircRNA\_100876 Is Upregulated in Gastric Cancer (GC) and Promotes the GC Cells' Growth, Migration and Invasion via miR-665/YAP1 Signaling.** Frontiers in genetics 2020, **11**:546275.
46. Zhou LH, Yang YC, Zhang RY, Wang P, Pang MH, Liang LQ: **CircRNA\_0023642 promotes migration and invasion of gastric cancer cells by regulating EMT.** European review for medical and pharmacological sciences 2018, **22**(8):2297–2303.

## Figures

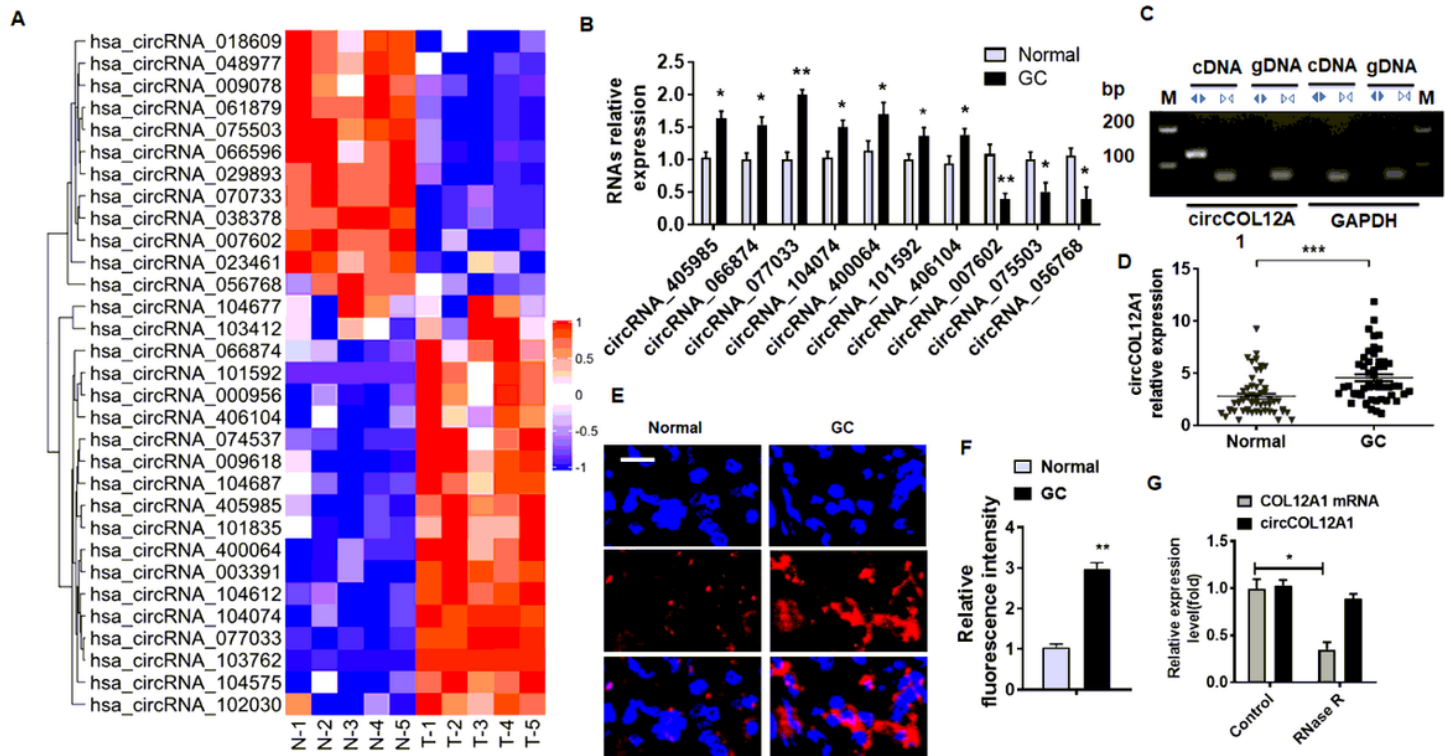
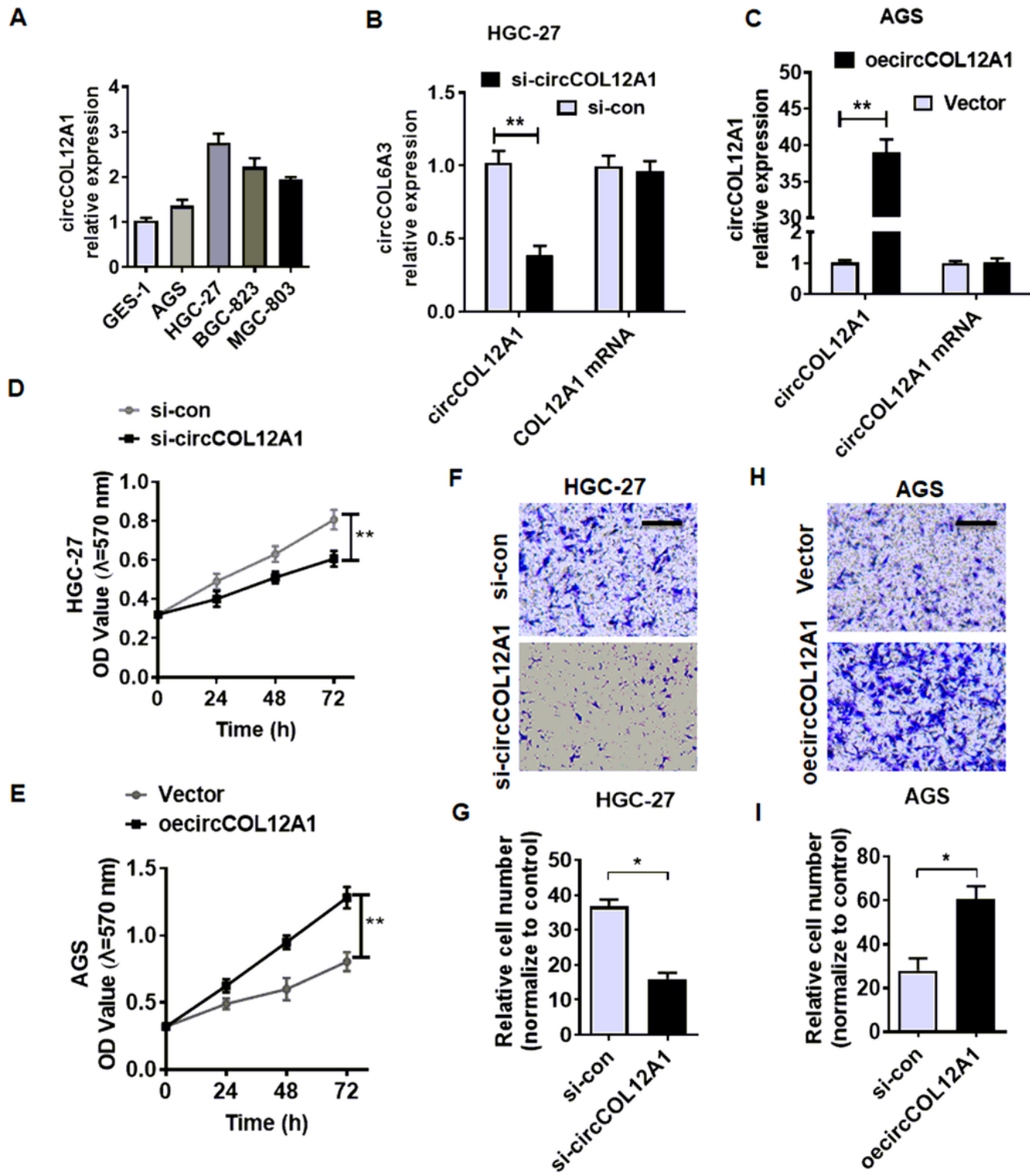


Figure 1

**Analysis of circular RNA expression in human GC tissues.** (A) Differential circRNA expression profiles in Normal (N) and Tumor (T) tissues. Heat map of hierarchical clustering indicates differentially expressed circRNAs (red: upregulation; blue: downregulation). A number in the right side represents a circular RNA. (B) Convergent or divergent primers were used to verify the expression of circRNAs from (A) via reverse transcription (RT)-PCR in gastric cancer and normal tissue. (C) circCOL12A1 (hsa-circRNA-0077033) was amplified by divergent primers in cDNA but not genomic DNA (gDNA) and linear control gene GAPDH. bp: size markers (in base pairs). (D) qRT-PCR analysis of circCOL12A1 expression in GC ( $n = 52$ ) and normal gastric tissues ( $n = 52$ ) normalized to GAPDH. (E and F) A fluorescence in situ hybridization assay was used to examine the expression and subcellular localization of circCOL12A1. Nuclei were stained with 4,6-diamidino-2-phenylindole (DAPI). Scale bars = 20  $\mu\text{m}$ . (G) Results of qRT-PCR analysis of circCOL12A1 and COL12A1 mRNA after treatment with RNase R in HGC-27 cells. All data are expressed as the mean  $\pm$  SEM from three independent experiments. \* $P < 0.05$ , \*\* $P < 0.01$  vs. the corresponding controls.



**Figure 2**

**circCOL12A1 plays an essential role in GC cell proliferation and migration.** (A) qRT-PCR analysis of the expression of circCOL12A1 in normal human gastric epithelial cells (GES-1 cell line) and cultured GC cell lines (AGS, HGC-27, BGC-823, and MGC-803). (B and C) HGC-27 (B) and AGS (C) cells were transfected with si-con, si-circCOL12A1, or an overexpression plasmid (oecircCOL12A1), and qRT-PCR analysis was conducted to measure circCOL12A1 expression. (D and E) HGC-27 and AGS cells were transfected as

above with the indicated RNA and plasmid, and cell viability was measured by an MTT assay. (F-I) Cells were prepared as in (D and E) and cell migration was measured by a transwell assay. All data are expressed as the mean  $\pm$  SEM from three independent experiments. \*P < 0.05, \*\*P < 0.01 vs. the corresponding controls.

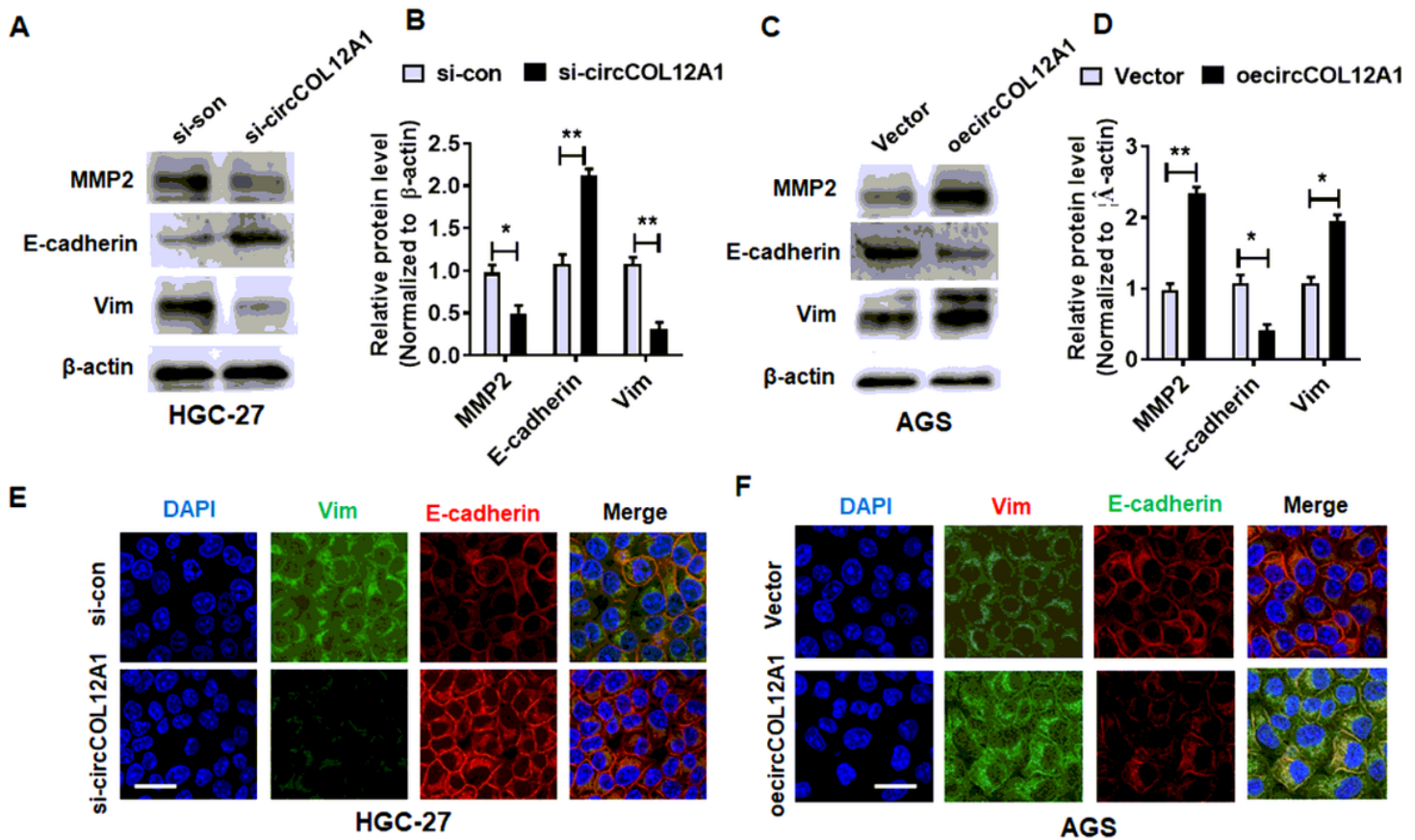


**Figure 3**

**circCOL12A1 promotes GC Cell EMT by regulating EMT-related genes.** (A and B) Western blot analysis was used to measure MMP2, vimentin, and E-cadherin protein levels in HGC-27 cells after transfecting with si-circCOL12A1 or control siRNA (si-con).  $\beta$ -actin was used as an internal control. (C and D) AGS cells were transfected with a circCOL12A1 (circ-pcDNA3.1-circCOL12A1) overexpression vector or control vector (circ-pcDNA3.1). Western blot analysis was used to measure MMP2, E-cadherin, and Vim protein levels. (E and F) HGC-27 (E) cells were transfected with si-con or si-circCOL12A1 and (F) AGS were transfected with the overexpression plasmid. Immunofluorescence staining was used to examine E-cadherin and Vim expression. Scale bars = 20  $\mu$ m. All data are expressed as the mean  $\pm$  SEM from three independent experiments. \*P < 0.05, \*\*P < 0.01 vs. the corresponding controls.

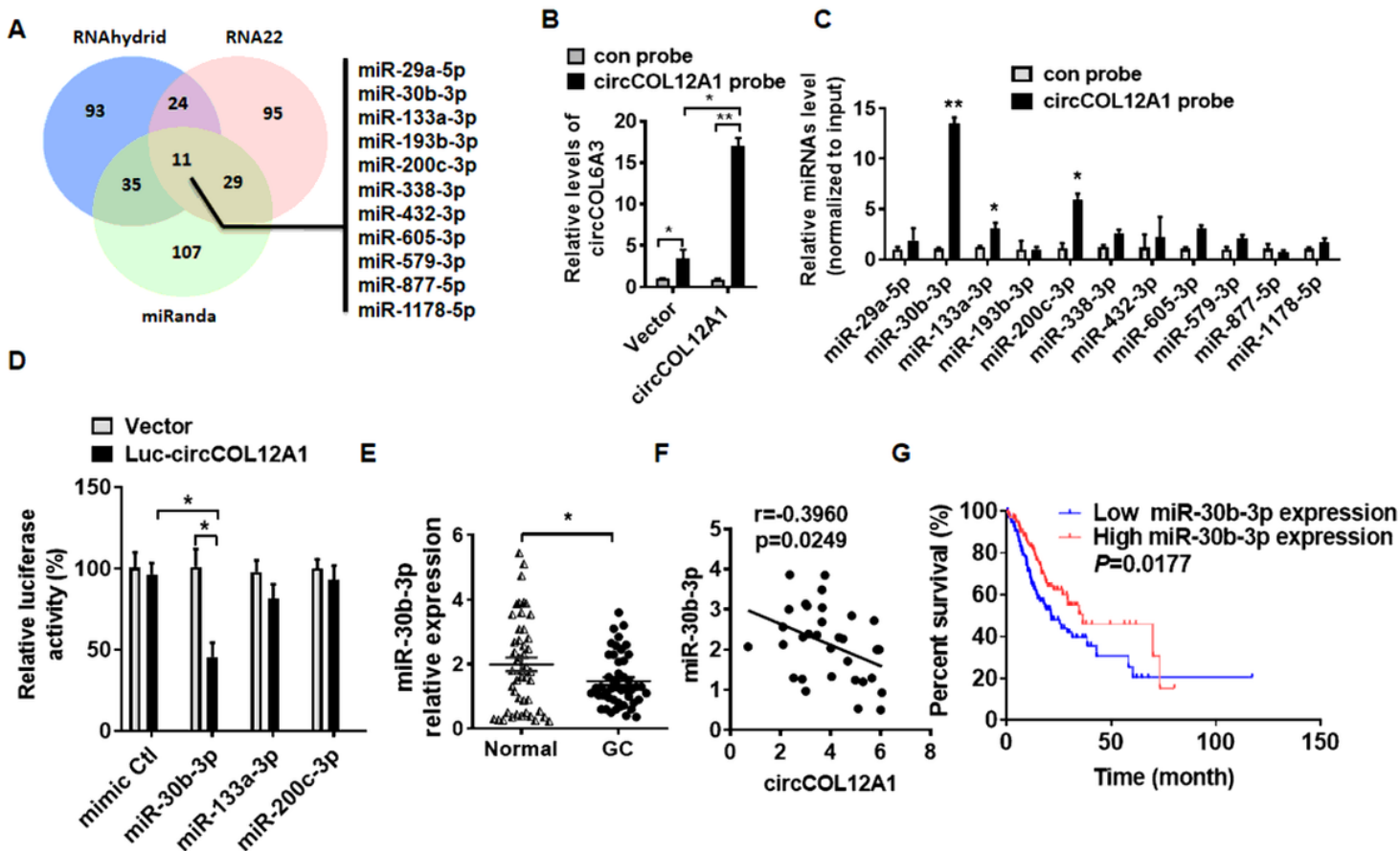


**Figure 4**

**circCOL12A1 sponges miR-30b-3p in GC cells.** (A) Candidate microRNAs (miRNAs) that interact with circCOL12A1 were predicted by three different target prediction programs and analyzed by a Venn diagram. (B) circ-pcDNA3.1-circCOL12A1 or control vectors were transfected into HGC-27 cells. qRT-PCR analysis was used to determine the pull-down efficiency of circCOL12A1 or the NC probe. (C) qRT-PCR was used to examine the enrichment of the indicated miRNAs in the pull-down precipitates, which were normalized to an internal control, U6. (D) HGC-27 cells were co-transfected with miR-30b-3p, miR-150-5p, or miR-181-5p mimic and the circCOL12A1-luciferase reporter (WT). Luciferase reporter assays were used to detect luciferase activity. (E) The expression of miR-30b-3p was measured via qRT-PCR in GC tissues and normal gastric tissues. (F) Relationship between miR-30b-3p expression and circCOL12A1 levels in GC tissue as determined by Spearman's correlation analysis ( $R = -0.4060$ ,  $P = 0.0211$ ). (G) Overall survival and miR-30b-3p levels in GC patients from the TCGA database exhibiting low ( $n = 100$ ) or high ( $n = 100$ ) expression were analyzed using Kaplan–Meier plots. All data are expressed as the mean  $\pm$  SEM from three independent experiments. \* $P < 0.05$ , \*\* $P < 0.01$  vs. the corresponding controls.

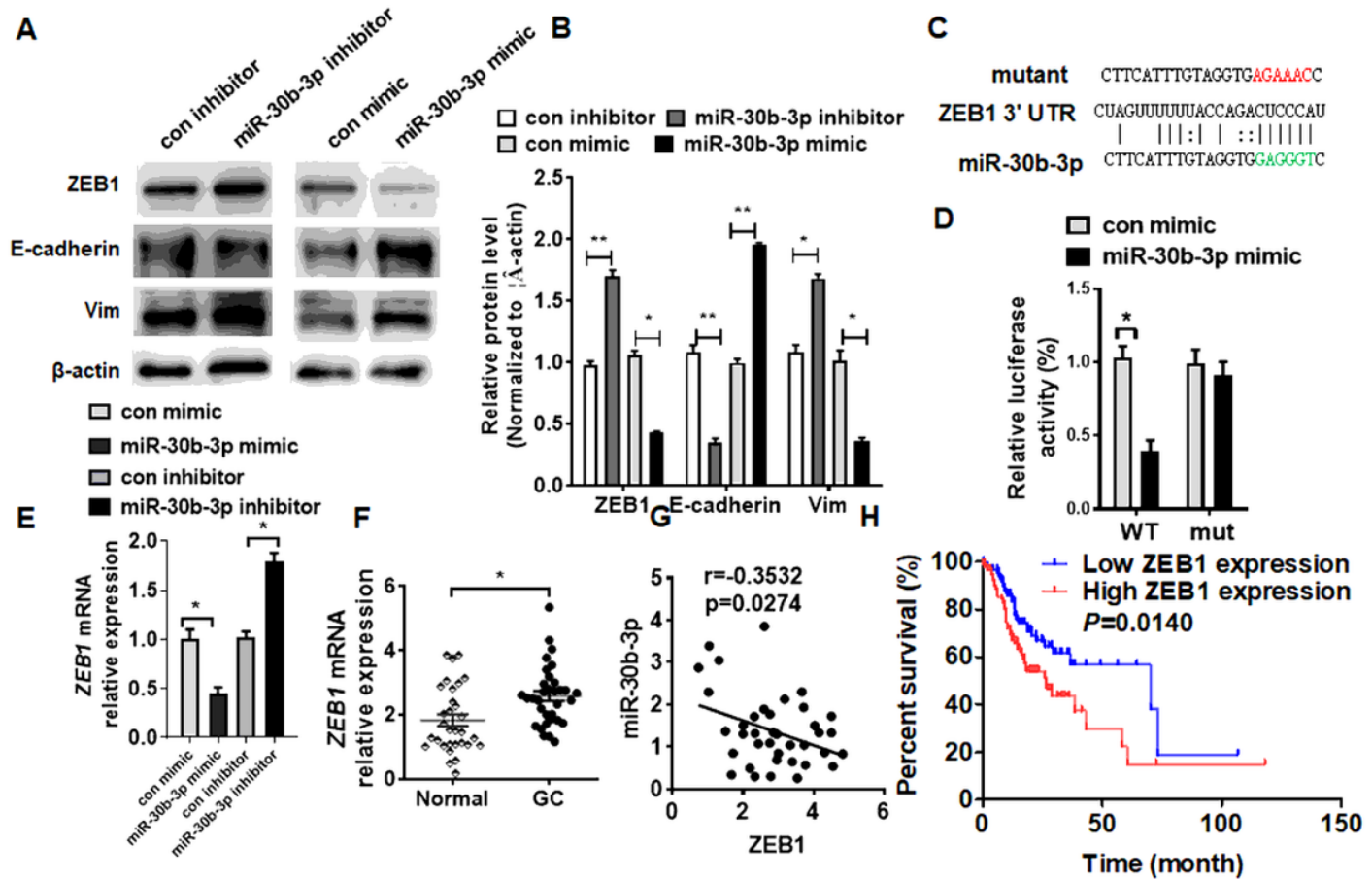


**Figure 5**

**miR-30b-3p suppresses GC cell EMT and migration by directly targeting the 3'UTR of the ZEB1 gene.** (A and B) HGC-27 cells were transfected with miR-30b-3p mimic, miR-30b-3p inhibitor, or its corresponding control. ZEB1, Vim, and E-cadherin protein levels were measured by western blot analysis and β-actin was used as an internal control. (C) Prediction of the miR-30b-3p binding site in the 3'-UTR of ZEB1. (D) HGC-27 cells were co-transfected with the miR-30b-3p mimic and ZEB1 3'-UTR-luciferase reporter (WT/mut) construct and luciferase reporter assays were performed. (E) HGC-27 cells were transfected with miR-30b-3p mimic, miR-30b-3p inhibitor, or its corresponding control, and qRT-PCR analysis was used to measure ZEB1 mRNA. (F) ZEB1 mRNA was measured via qRT-PCR in GC tissues and normal gastric tissues and normalized against β-actin. (G) The relationship between miR-30b-3p expression and ZEB1 mRNA expression in GC tissues was analyzed via Spearman's correlation analysis ( $R = -0.3532$ ,  $P = 0.0274$ ). (H) Overall survival of GC patients from the TCGA database relative to miR-30b-3p expression was analyzed using a Kaplan–Meier plot. All data are expressed as the mean  $\pm$  SEM from three independent experiments. \* $P < 0.05$ , \*\* $P < 0.01$  vs. the corresponding controls.

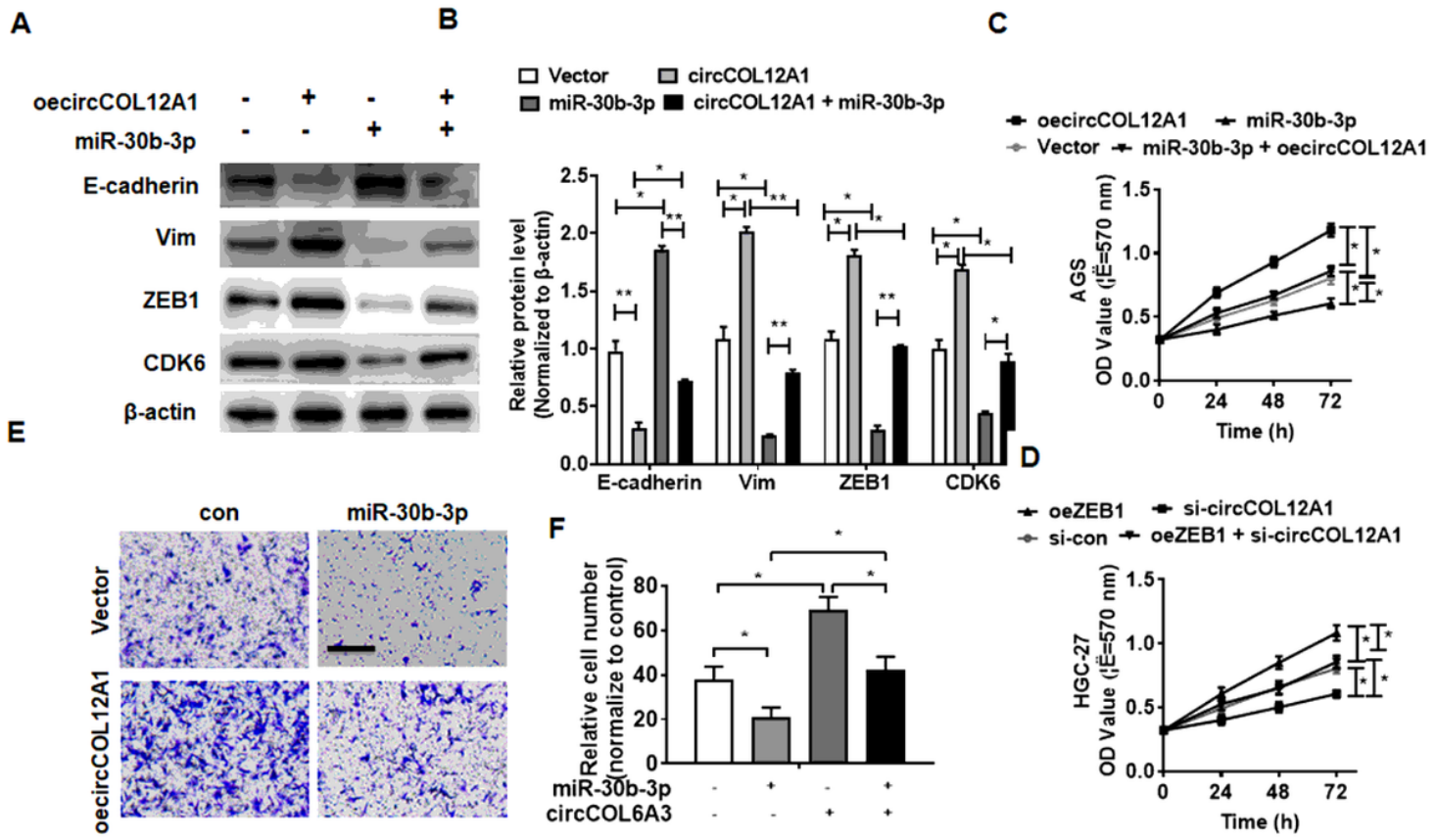


**Figure 6**

**circCOL12A1/miR-30b-3p/ZEB1 axis regulates GC cell migration and EMT. (A and B)** AGS cells were transfected with overexpressing circCOL12A1 or miR-30b-3p mimics, or co-transfected with overexpressing circCOL12A1 and miR-30b-3p mimic vectors simultaneously. ZEB1, Vim, and E-cadherin protein levels were detected by western blot analysis. **(C)** AGS cells were prepared as in (A) and cell viability was evaluated by MTT assay. **(D)** HGC-27 cells were transfected with si-circCOL12A1 or overexpressing ZEB1 vectors, or co-transfected with si-circCOL12A1 and overexpressing ZEB1 vectors simultaneously. Cell viability was evaluated by MTT assay. **(E and F)** AGS cells were prepared as in (a) and cell migration was evaluated by a Transwell migration assay. All data are expressed as the mean ± SEM from three independent experiments. \*P < 0.05, \*\*P < 0.01 vs. the corresponding controls.

## Supplementary Files

This is a list of supplementary files associated with this preprint. Click to download.

- [SupplementaryTable1DifferentiallyExpressed.xls](#)